This paper is part of the following report:

TITLE: Verification and Validation Data for
Computational Unsteady Aerodynamics [Donnees de
verification et de valadation pour
l'aerodynamique instationnaire numerique]

To order the complete compilation report, use: ADA390566

# 16C. LARGE-AMPLITUDE, HIGH-RATE ROLL OSCILLATIONS OF A 65° DELTA WING AT HIGH INCIDENCE

Neal M. Chaderjian and Lewis B. Schiff
NASA Ames Research Center
Moffett Field, California, U.S.A.

## INTRODUCTION

The IAR/WL 65° delta wing experimental results provide both detail pressure measurements and a wide range of flow conditions covering from simple attached flow, through fully developed vortex and vortex burst flow, up to fully-stalled flow at very high incidence. Thus, the Computational Unsteady Aerodynamics researchers can use it at different level of validating the corresponding code. In this section a range of CFD results are provided for the 65° delta wing at selected flow conditions. The time-dependent, three-dimensional, Reynolds-averaged, Navier-Stokes (RANS) equations are used to numerically simulate the unsteady vortical flow. Two sting angles and two large-amplitude, high-rate, forced-roll motions and a damped free-to-roll motion are presented. The free-to-roll motion is computed by coupling the time-dependent RANS equations to the flight dynamic equation of motion. The computed results are compared with experimental pressures, forces, moments and roll angle time history. In addition, surface and off-surface flow particle streaks are also presented.

## LIST OF SYMBOLS AND DEFINITIONS

| | |
|---|---|
| B | wing span, (in) |
| c | root chord, (in) |
| $c_0$ | mean aerodynamic chord, (in) |
| $C_p$ | pressure coefficient $=(p-p_0)/qs$ |
| $C_\ell$ | rolling moment coefficient $=\ell/qsB$ |
| $C_N$ | normal force coefficient $=N/qs$ |
| f | frequency, (Hz) |
| k | reduced frequency $=\pi fB/V_0$ |
| $\ell$ | rolling moment, (lbs-in) |
| $M_\infty$ | Mach number |
| m | pitching moment, (lbs-in) |
| N | normal force, (lbs) |
| n | yawing moment, (lbs-in) |
| p | pressure, (psi) |
| $p_0$ | static pressure, (psi) |
| q | dynamic pressure, (psi) |
| Re | Reynolds number, based on root chord |
| s | wing area, (in$^2$) |
| S | semi span, (in) |
| $T_0$ | static temperature, (°C) |
| t | time (sec) |
| $V_0$ | free stream velocity (ft/sec) |
| x,y,z | body axes coordinates |
| $X_{Cp}$ | center of pressure in x axis, (in) |
| $\alpha$ | angle of attack, (°) |
| $\sigma$ | sting angle (between body axis and tunnel axis), (°) |
| $\phi$ | roll angle, (°) |
| $\phi_0$ | mean roll angle or initial roll angle, (°) |
| $\Delta\phi$ | amplitude, (°) |

| $\dot{\phi}$ | roll angular rate, (rad/sec) |
|------|------|
| CCW | counter clockwise |
| CW | clockwise |
| CFD | Computational Fluid Dynamics |
| NSS | Navier-Stokes Simulation |
| RANS | Reynolds-averaged, Navier-Stokes Equations |

# FORMULARY

## General Description of model

| 1.1 | Designation | IAR Delta Wing |
|-----|-------------|----------------|
| 1.2 | Derivation | IAR Dynamic Experimental Model |
| 1.3 | Type | Full model |
| 1.4 | References | Ref. 1 (Fig. 1) |

## Model Geometry

| 2.1 | Planform | Delta wing-body, See Fig. 1 |
|-----|----------|------------------------------|
| 2.2 | Aspect ratio | 1.866 |
| 2.3 | Mean aerodynamic chord | 16.323 in |
| 2.4 | Root chord | 24.485 in |
| 2.5 | Span | 22.835 in |
| 2.6 | Reference center | 13.875 aft of the apex |
| 2.7 | Leading edge sweep | 65° |
| 2.8 | Trailing edge sweep | 0° |
| 2.9 | Taper ratio | 0 |
| 2.10 | Twist | 0° |
| 2.11 | Dihedral | 0° |
| 2.12 | Area of planform | 279.486 in$^2$ |
| 2.13 | Leading-edge bevel (leeward) | 9° (perpendicular to leading-edge) |
| 2.14 | Leading-edge bevel (windward) | 9° (perpendicular to leading-edge) |
| 2.15 | Trailing edge bevel (leeward) | 9° (perpendicular to trailing edge) |
| 2.16 | Trailing edge bevel (windward) | 9° (perpendicular to trailing edge) |
| 2.17 | Leading-edge radius | 0.020 in |
| 2.18 | Tolerance of leading-edge radius | ±10% |
| 2.19 | Definition of profiles | 0.375 inch thick flat-plate wing with double-bevelled (18° included angle) sharp leading and trailing edge |
| 2.20 | Center body | Ogive-cylinder |
| 2.21 | Form of wing-body junction | Bevelled, see Fig. 1 |
| 2.22 | Form of wing tip | Sharp |
| 2.23 | Control surface details | None |
| 2.24 | Center-body diameter | 3.150 in |
| 2.25 | Radius of forebody | $r = \sqrt{24.103^2 - (12.243 - x)^2} - 22.528$ in |
| 2.26 | References | Ref. 1 (Fig. 1) |

## CFD Grid Details

| | | |
|---|---|---|
| 3.1 | RANS grid size | 67 axial x 209 circumferential x 49 normal points (baseline grid); 113 x 421 x 97 points (finest grid), See Fig. 2 |
| 3.2 | Additional Remarks | Full-body grids used in all cases; zonal grids used in axial directio to fit machine memory; zonal boundaries are one-to-one matching |

## CFD Code used

| | | |
|---|---|---|
| 4.1 | RANS code | Novier-Stokes Simulation (NSS) code, Beam-Warming, block or diagonal, central differencing, blended 2nd- and 4th-order dissipation, reduced dissipation in boundary layer |
| 4.2 | Turbulence model | Baldwin-Lomax with Degani-Schiff modifications, no fixed transition |
| 4.3 | Computational time step | $3.62 \times 10^{-3} < \tau < 5.0 \times 10^{-3}$, $6.67 \times 10^{-6}$ sec $< \Delta t < 9.0 \times 10^{-6}$ sec |
| 4.4 | Computation time | 80 hours per oscillation cycle on a CRAY C-90 single processor - block version (15,000 steps per cycle of oscillation) |
| 4.5 | Additional remarks | Unsteady computation started with steady solution at $\phi_{max}$. Solution converged after 2-3 cycles |
| 4.6 | Reference on code | Ref. [5] |

## Model Motion

| | | |
|---|---|---|
| 5.1 | Mode of applied motion | Sinusoidal roll oscillations and free-to-roll motion about longitudinal axis of symmetry |
| 5.2 | Range of amplitude | $28.2°, 31.9°, 40.0°$ |
| 5.3 | Reduced frequency | $f = 7$ Hz, $10$ Hz; $k = 0.14, 0.20$ |
| 5.4 | Additional Remarks | oscillations about $\phi_0 = 0.0°, 28.0°$ |

## Boundary Conditions

| | | |
|---|---|---|
| 6.1 | Mach Number | 0.27 |
| 6.2 | Reynolds Number | $Re_c = 3.67 \times 10^6$, based on root chord |
| 6.3 | Temperature | $300°$ K |
| 6.4 | Range of model incidence | $15°$ and $30°$ |
| 6.5 | Definition of model incidence | Model incidence defined relative to model axis of symmetry |
| 6.6 | Additional Remarks | Distance of far field boundary is 5 root chords normal to wing, 2 root chords upstream and downstream of wing |

## Data Presentation

| | | |
|---|---|---|
| 7.1 | Static Cases | Roll moment versus roll angle |
| | | Normal force versus roll angle |
| | | Center of pressure versus roll angle |
| | | Leeward surface pressure distributions for various roll angles |
| | | Surface flow patterns for various roll angles |
| | | Vortex breakdown point versus roll angle |
| 7.2 | Forced Roll Oscillations | Instantaneous roll moment versus roll angle |
| | | Instantaneous normal force versus roll angle |
| | | Center of pressure versus roll angle |
| 7.3 | Free-to-Roll Oscillations | Roll angle history versus time |
| 7.4 | Sample illustrations | Fig. 3 to Fig. 10 |

| 7.5 | Additional Remarks | All above quantities are compared against IAR experiments (Case No. 2, No. 3, No. 5, No. 6 and No. 10) |

## Personal contact for further information

Dr. Neal M. Chaderjian, T27B-2, NASA Ames Research Center, Moffett Field, California U. S. A

Phone: (650) 604-4472, E-mail: nchaderjian@mail.arc.nasa.gov

## List of references

[1]. N. M. Chaderjian, "Navier-Stokes Prediction of Large-Amplitude Delta-Wing Roll Oscillations," *Journal of Aircraft*, Vol. 31, No. 6, pp. 1333-1340.

[2]. N. M. Chaderjian and L. B. Schiff, "Navier-Stokes Prediction of a Delta Wing in Roll with Vortex Breakdown," AIAA Paper 93-3495, 11th Applied Aerodynamics Conference, Monterey CA, August 1993.

[3]. N. M. Chaderjian and L. B. Schiff, "Numerical Simulation of Forced and Free-to-Roll Delta-Wing Motions," *Journal of Aircraft*, Vol. 33, No. 1, pp. 93-99.

[4]. N. M. Chaderjian and L. B. Schiff, "Navier-Stokes Analysis of a Delta Wing in Static and Dynamic Roll," AIAA Paper 95-1868, 13th Applied Aerodynamics Conference, San Diego, CA, June 1995.

[5]. N. M. Chaderjian, "Comparison of Two Navier-Stokes Codes for Simulating High-Incidence Vortical Flow", *Journal of Aircraft*, Vol. 30, No. 3, pp. 357-364.

[6]. E. S. Hanff and X. Z. Huang, "Roll-Induced Cross-Loads on a Delta Wing at High Incidence," AIAA Paper 91-3223, September 1991

[7]. E. S. Hanff and S.B. Jenkins, "Large-Amplitude High-Rate Roll Experiments on a Delta and Double Delta Wing," AIAA paper 90-0224, January 1990.
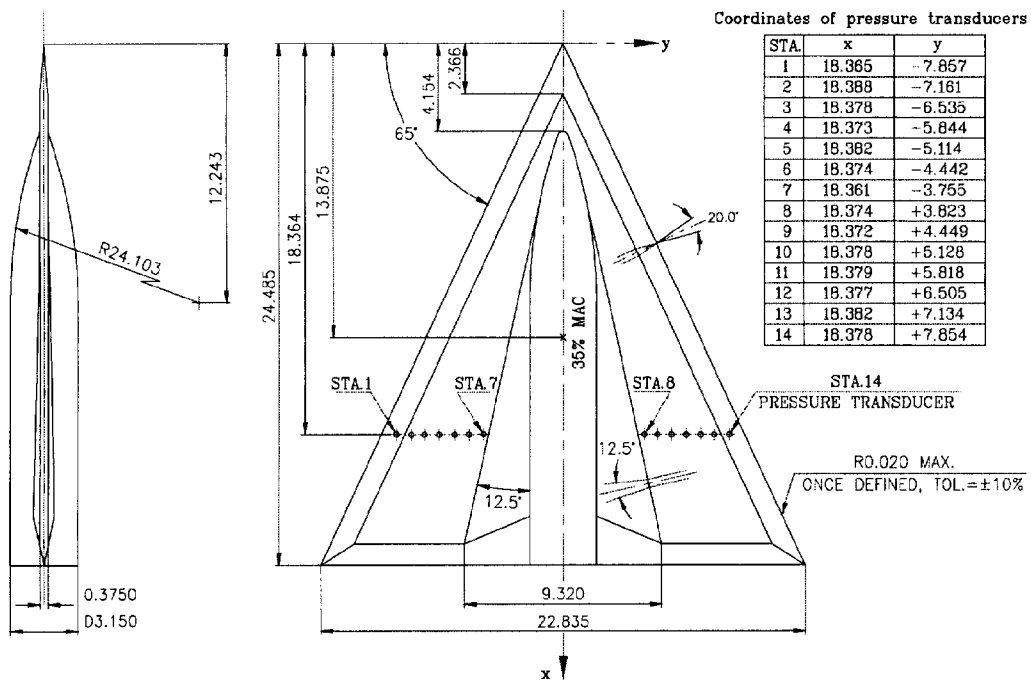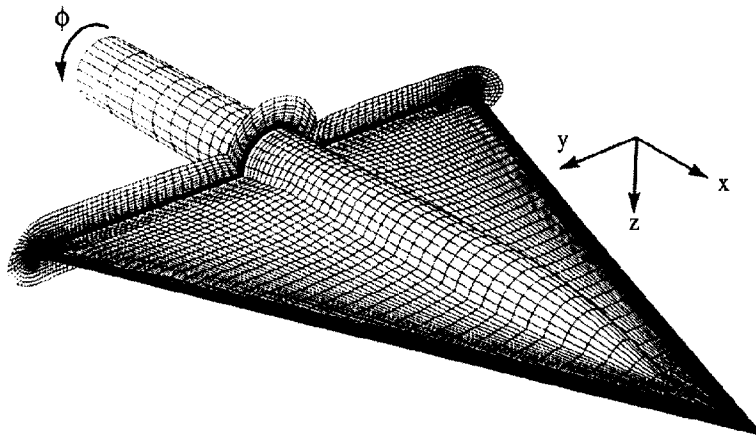
Coordinates of pressure transducers

| STA. | x | y |
|---|---|---|
| 1 | 18.365 | -7.857 |
| 2 | 18.388 | -7.161 |
| 3 | 18.378 | -6.535 |
| 4 | 18.373 | -5.844 |
| 5 | 18.382 | -5.114 |
| 6 | 18.374 | -4.442 |
| 7 | 18.361 | -3.755 |
| 8 | 18.374 | +3.823 |
| 9 | 18.372 | +4.449 |
| 10 | 18.378 | +5.128 |
| 11 | 18.379 | +5.818 |
| 12 | 18.377 | +6.505 |
| 13 | 18.382 | +7.134 |
| 14 | 18.378 | +7.854 |



Fig. 1 65° delta wing model



Fig. 2 Perspective view of the computational grid
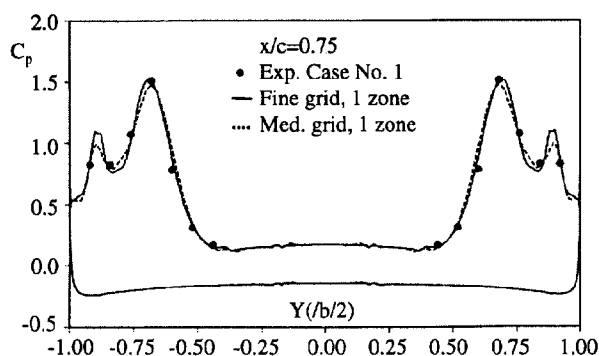
Fig. 3 Effects of grid refinement and zonal boundary condition treatment on the pressure coefficients
$M_\infty=0.27$, $\alpha=15°$, $\phi=0$, Re=3.67 million
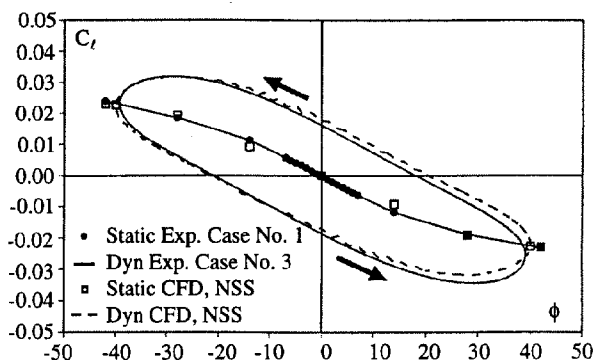


Fig. 4 Comparison of computational and experimental rolling moment coefficients for dynamic and static cases
$M_\infty=0.27$, $\sigma=15°$, $\Delta\phi=40°$, k=0.14, Re=3.67 million
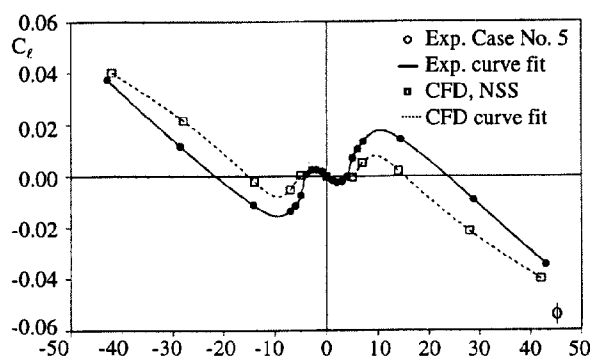


Fig. 5 Comparison of mean computed and experimental rolling moment coefficients for static roll angles
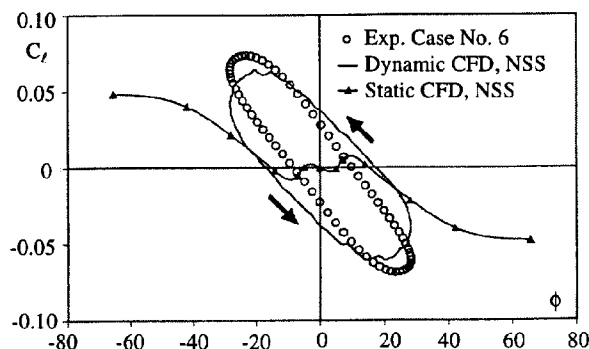$M_\infty=0.27$, $\sigma=30°$, Re=3.67 million



Fig. 6 Dynamic and static rolling-moment coefficients
$M_\infty=0.27$, $\sigma=30°$, $\phi_0=0°$, $\Delta\phi=28.2°$, k=0.20, Re=3.67 million
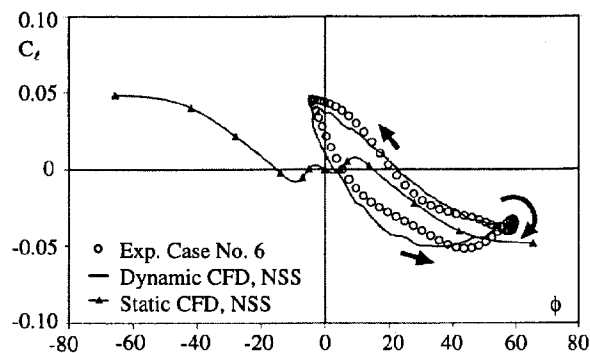


Fig. 7 Dynamic and static rolling-moment coefficients
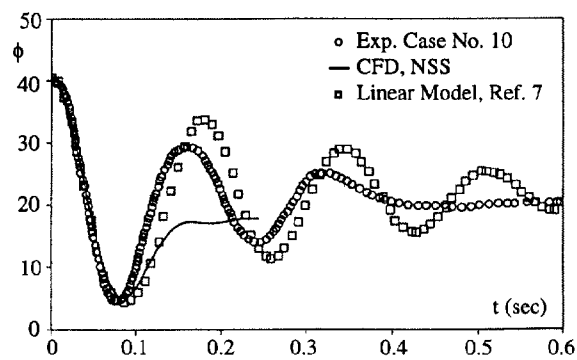$M_\infty=0.27$, $\sigma=30°$, $\phi_0=28°$, $\Delta\phi=31.9°$, Re=3.67 million



Fig. 8 Time history of roll angle for free-to-roll motion
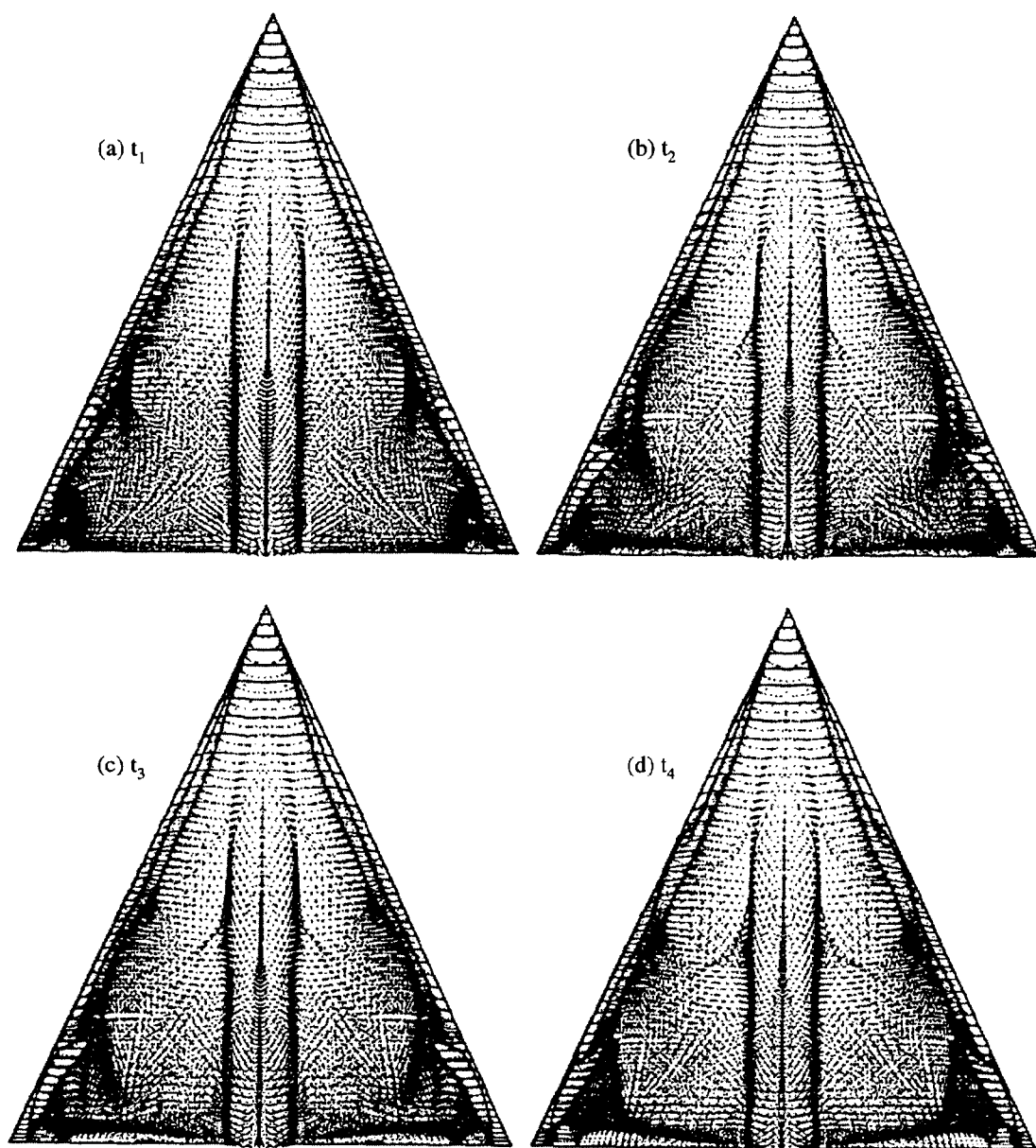$M_\infty=0.27$, $\sigma=30°$, $\phi_0=40.5°$, Re=3.67 million

Fig. 9 Computed unsteady surface-flow particle-streaks at four sequential times
$M_\infty=0.27$, $\alpha=30°$, $\phi=0°$, Re=3.67 million
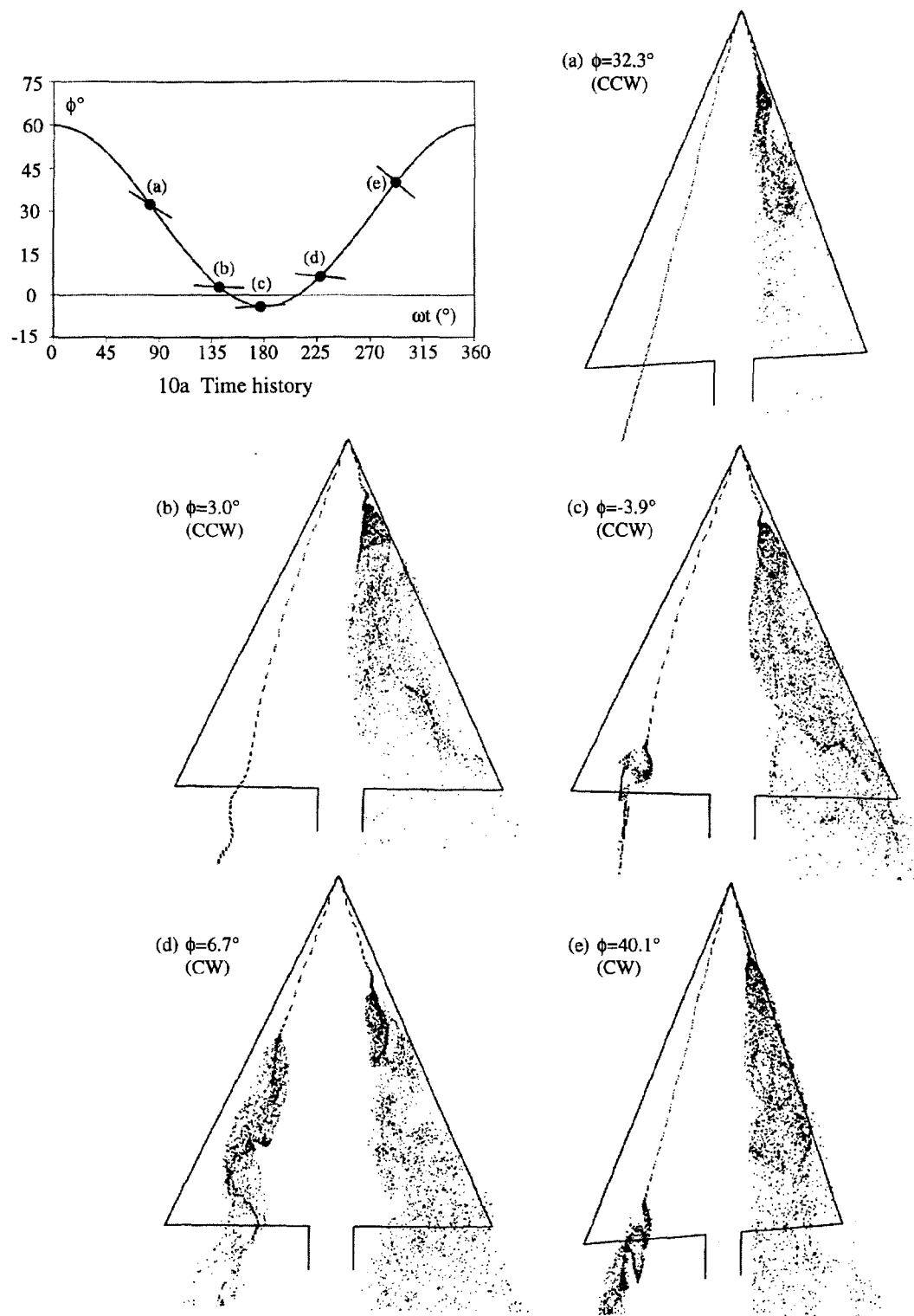
Fig. 10 Periodic formation and disappearance of vortex breakdown over left wing
$M_\infty=0.27$, $\alpha=30°$, $\phi_0=28°$, $\Delta\phi=31.9°$, k=0.20, Re=3.67 million